First Asia Pacific Conference on Advanced Research (APCAR-2015)
ISBN: 978 0 994 3656 68
www.apiar.org.au

BIOLOGICALLY INSPIRED VECTOR FIELDS TO GENERATE HAIR DIRECTIONS

Siew Mai Bong & Shaun Bangay
Deakin University, Australia
Corresponding Author: m.bong@research.deakin.edu.au

Abstract

This paper describes how biologically inspired vector fields can be used to partially automate the manual and time-consuming process of specifying hair directions. This approach replicates the consequence of stretching of skin from natural hair development process, in contrast to replicating the appearance of hair. The direction of each hair on the surface of an arbitrary 3D model is determined by interpolating the solution vector field that satisfies a set of user-defined constraints describing the stretching of skin. Results found that the generated hair directional pattern closely resembles that found naturally. Further investigation revealed that the presence of naturally occurring hair types and the varying distribution of hair directions induced by the calculated vector field enhanced the realism of hair coats generated using this approach. Aside from hair or fur, this approach can also be applied to hair-like masses such as grass, feathers, or scales.

Keywords: biologically inspired, computer graphics, fur, procedural generation, vector fields

Introduction

Hair, fur, or feather coats found naturally on animals play an important role in communication as well as reflecting their overall health. However, reproducing these coats is a challenging task in computer graphics (CG) due to their sophisticated structure. The focus of this research is to partially automate the process of replicating natural hair directions using biologically inspired vector fields. The results will be compared to the natural hair coats of wild-type mice for they are well studied in biological literature.

Figure 1**Error! Reference source not found.**, reproduced from Figure 2A of [1], shows the four different types of mouse hair found naturally on wild-type mice: guard (g), awl (a), auchene (au), and zigzag (z), which covers about 2.3%, 24.4%, 1.9%, and 71.5% of its body [2]. Note the different hair shapes (top) and diameters (bottom) of the hair types as shown in Figure 1. Guard hairs are long and fairly straight, awl hairs are shorter, auchene hairs have a sharp bend, and zigzag hairs are thin and have three to four alternating sharp bends [1].

Figure 1 Different mouse hair types.

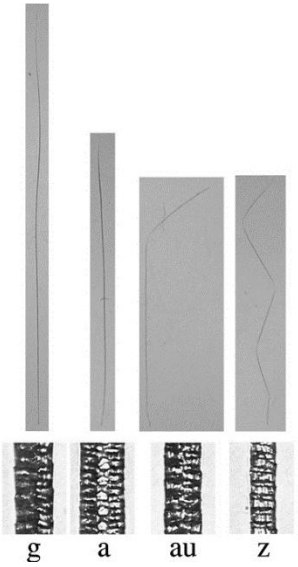

The stretching of skin during hair development causes hairs to slope in the direction of this stretch [3]. For a mouse, the skin stretches from its nose towards its tail. Since hairs originate from hair follicles, their characteristics depend on the properties of their corresponding hair follicles. As a result, hair density varies over different regions of its body due to the varying hair follicle density, where the average number of hair follicles in the neck, shoulder, back, legs, and belly regions are

73.8, 69.6, 63.2 61.5, and 59.6 hairs per square millimetre respectively [4].
From genetically modifying mice, it is found that changes to the hair follicle size affects the resulting hair diameter and length as well [1]. Assuming that there is a relationship between sizes of hair and hair follicle, apart from directly extracting the hair positions from the results of simulating a reaction-diffusion model for mouse hair follicle formation [5]. Distributions of hair diameters and lengths are derived from scaling the distribution of hair follicle diameter to fit experiment data from 6 to 8 week old mice [6].

Confronted by the large number of hairs, each with different shapes and sizes, it is exceedingly laborious to manually sculpt these hairs individually. To overcome this problem, various methods have been proposed to assist in hair modelling [7]. A geometry-based method improves the user interface so that hairs can be edited in groups, while an image-based method reconstructs hair from multiple images. Finally, physically based methods render hair by simulating a model that takes a few parameters as input.

One of these physically-based methods use vector fields to shape human hair [8]. With a statistical wisp model, hair types are defined using a master hair strand. Then, member hair strands are formed from the master hair strand with varying shapes, lengths, and distances from the master strand. After specifying the hairs, force fields are used to shape them. These force fields could also be constrained to form complex hairstyles such as braids. However, the aforementioned approach focuses on replicating the appearance of natural hair, not the modelling the cause of natural hair directions.

This paper describes a physically based method to partially automate the generation of hair directions by modelling the results of the natural hair development process using constrained vector fields. This approach combines the stretching of skin during natural hair development [3], natural hair types [1], and distributions of hair properties that mimic natural ones [6] to generate hair coats. The process is demonstrated using the hair coat of wild-type mice to determine how well the generated hair coat can replicate a natural mouse hair coat. Specifically, the criteria for evaluation are how natural the generated hair types and directions are and how this approach behaves with different 3D models. Results indicate that the hair directional pattern in the generated hair coat closely matches that of a natural hair coat. In addition, the variation to the structure of individual hairs gives a fuzzy silhouette to the mouse similar to that found naturally. Furthermore, it is found that this approach can be applied to arbitrary 3D models and the amount of time taken to generate the hair coat is proportional to the complexity of the model as well as the hair count.

Related Work

One of the earliest representations is the particle system [9], where the paths travelled by particles could be rendered as individual hair strands. Although the representation is flexible, sculpting different hairstyles by explicitly modifying individual hair strands was difficult and time consuming. The manual process is either automated by capturing the overall hair shape of real fuzzy objects in 3D, or accelerated by improving the user interface, such as enabling the modification of hair strands in clusters, or introduction of force fields to model overall hair shape [7].

Recently, the most common approach to capture hairstyles is to reconstruct the geometry of individual hair fibres. Given a single colour image and a few user-defined strokes, the hairstyle is extracted from the image and reconstructed in 3D using heuristics to resolve for uncertainties [10]. This approach can be used to transfer hairstyles from one image to another in different

viewing angles. Using more than one colour image, curly hairstyles are captured by attempting to find the probable connections and directions [11]. This approach combined with hair simulation accommodates for strong outliers [12].
Through the use of multiple projectors and cameras, hairstyles with complex curls are captured in detail by capturing the six-dimensional hair reflectance field [13]. The problem of reconstructing hairstyles is further simplified through the use of thermal imaging [14], since only infrared radiation is captured. Images are not only unaffected by the effects of lighting, they also show clear boundaries between skin and hair. Other approaches deviate from capturing realism, such as synthesising new hairstyles from a given hairstyle [15], or generating hair meshes within volumes enclosed by polygonal surfaces [16]. Aside from human hair, the placement of feathers is automatically generated to prevent intersections between feathers [17].

Apart from hairstyles, facial hairs are reconstructed by detecting and tracing them individually from the multiple images capturing these hairs in different viewing angles [18]. However, there is a limit to how much is visible in the captured images, thus the hairs are reconstructed on the visible surface, not the true surface. Another approach captures hair fibres on turntable for high quality results.

So far, previous works address the problem of replicating hair appearance, not the consequence of stretching of skin during hair development, which is the problem this paper shall investigate.

Method

This section describes the process of calculating the vector field that will act as the consequence of stretching of skin during hair development.

Firstly, the user will place a set of constraints on the tangent vector field [19] so that it imitates the consequence of the stretching of skin during hair development. These constraints are specified in Equation 1, where its solution c_e is the vector field.

In summary, constraints on the vector field can be defined on any combination of vertices, edges or triangles on a given user-defined 3D model (or simplicial complex) as s_v, c_z or r_t in Equation 1 respectively. A positive or negative vertex constraint will result in a sink or a source, while a positive or negative edge constraint will guide the vector field along or against the direction of the edge, and finally, a positive or negative triangle constraint will result in a vortex that follows or opposes the orientation of the triangle.

Since the user-defined simplicial complex may be low in resolution, the solution vector field with the given set of constraints is interpolated before it is used to determine hair directions.

Generating Hair Directions

Let κ be a user-defined simplicial complex consisting of a set of 0-simplices or vertices $S_0(\kappa)$, a set of 1-simplices or edges $S_1(\kappa)$, and a set of 2-simplices or triangles $S_2(\kappa)$.

Given the user-defined 3D model, the tangent vector field is defined as the discrete 1-form c_e of a 1-simplex $e \in S_1(\kappa)$ is a $n \times 1$ matrix found by solving equation 6 of [19]

Equation 1

$$(M + Z^T W Z)c_e = \star_1 \delta_2 r_t + \star_1 d_0 s_v + Z^T W c_z$$

ISBN: 978 0 994 3656 68

, where M is a $n \times n$ matrix and $M = d_1^T \star_2 d_1 + \star_1 d_0 \star_0^{-1} d_0^T \star_1$ from equation 1 of [19], δ_k is the boundary matrix for k-form [20], d_k is the co-boundary matrix for k-form, $\star_k$ is the diagonal Hodge-star matrix for k-form, Z is the $n \times n$ matrix of edges to be constrained, W is a diagonal matrix containing the weights of edge constraints, and c_z is a $n \times 1$ matrix containing the values of the edge constraints.

Given that the constraints on tangent vector field are designed so that it mimics the consequence of stretching of skin, the first step to interpolate this tangent vector field is to use it to specify the hair directions for all vertices found in the 3D model. Given areal coordinates $(\alpha_i, \alpha_j, \alpha_k)$ on 2-simplex $t_{ijk} \in S_2(\kappa)$, where α_x is an areal coordinate corresponding to 0-simplex $v_x \in S_0(t_{ijk})$, rearranging equation 4 of [19], the hair direction vector field $\vec{u}$ is defined as

$$\vec{u} = -\frac{1}{2|t_{ijk}|}\begin{vmatrix} \vec{p}_{jk}^{\perp} & \vec{p}_{ki}^{\perp} & \vec{p}_{ij}^{\perp} \\ \alpha_i & \alpha_j & \alpha_k \\ c_{jk} & c_{ki} & c_{ij} \end{vmatrix}$$

, where $|t_{ijk}|$ is the intrinsic volume of t_{ijk}, c_{xy} is the discrete 1-form of the 1-simplex $\vec{p}_{xy} \in S_1(t_{ijk})$, $\vec{p}_{xy}^{\perp}$ is the normalised direction vector of the 1-simplex $\vec{p}_{xy}$ rotated by $\frac{\pi}{2}$ radians to the plane t_{ijk}.

Now, for each vertex in the 3D model, the hair direction(s) are averaged to interpolate the hair direction vector field. For all 2-simplices $t_{ijk} \in S_2(\kappa)$, the hair direction vector $\vec{u}$ is calculated for all 0-simplices $v_i, v_j, v_k \in S_0(t_{ijk})$. Since some 0-simplices $v_x \in S_0(\kappa)$ may be shared with two or more 2-simplices, then let N be the number of hair direction vectors acting on the m^{th} 0-simplex. By averaging the hair direction vectors, the interpolated hair direction vector for the m^{th} 0-simplex is $\vec{v} = \frac{1}{N}\sum_{i=1}^{N} \vec{u}_i$.

Finally, the unit hair direction vector $\hat{d}$ for a hair with areal coordinates $(\beta_i, \beta_j, \beta_k)$ on 2-simplex $t_{ijk} \in S_2(\kappa)$ is

$$\hat{d} = \frac{\beta_i \vec{v}_i + \beta_j \vec{v}_j + \beta_k \vec{v}_k}{|\beta_i \vec{v}_i + \beta_j \vec{v}_j + \beta_k \vec{v}_k|}$$

, where $\vec{v}_x$ is the interpolated hair direction vector of x^{th} 0-simplex of $S_0(t_{ijk})$.

Materials

Experiments are performed on a Microsoft Surface Pro 2 with Intel Core i5-4200U Quad-Core CPU @ 1.60 GHz and 4.00 GB RAM, running on Windows 8.1 Pro 64-bit operating system. The software Mathematica 9 is used to generate hair coats, while Blender is used for rendering.

Evaluation

This section describes the experiment environment and configuration to evaluate the criteria specified in the beginning of this paper.

ISBN: 978 0 994 3656 68
www.apiar.org.au

3D Model Specification

Four different user-defined 3D models are used to test the behaviour of the proposed method: a plane, icosphere, sphere and mouse. The plane represents the simplest case of a 3D model, while the icosphere and sphere represent a faceted and a fairly smooth mesh respectively. Lastly, the mouse represents a complex 3D model as well as a basis for evaluating how natural the generated hair types and hair directions are.

Design of Constraints on Vector Field

Edge, triangle and vertex are respectively applied on the first three 3D models to test if in all three cases, the hair directions are smoothed over the surface of the 3D model and obey the specified constraints. As it is known that the skin of a mouse stretches from its nose towards its tail during hair development [3], a source will be placed at its nose and a sink at its tail to mimic its consequence. Note that the generated hair coats of the 3D models use generated data that mimic distributions of mouse hair positions, diameters, and lengths [6]. Since the hair densities vary over different body regions of the mouse, for each of the five body regions (Figure 2), a different hair distribution is generated so that the hair density approximates the average hair density in that region [4] before it is sampled repetitively over that region.

Figure 2 Different body regions of the mouse.

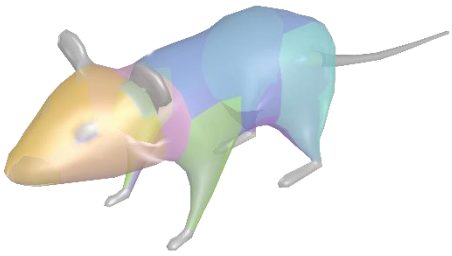

Comparison with Wind Force Field

A control experiment will question the significance of the steps taken in the proposed method. In place of the vector field, a force field to blow the hairs of the mouse from its head towards its tail. As for hair types, there will be only one, which is completely straight. Furthermore, the hair placement in the control experiment is randomly distributed over the surface of the 3D model. These three tests will determine if there are any significant differences in hair directions, hair types, and hair placement between the control experiment and proposed method.

Comparison with Natural Mouse Hair Coat

The hair coat generated from the proposed method will be flattened to compare its overall hair directional pattern with that of a natural mouse hair coat.

Results

Figure 3 shows four different user-defined simplicial complexes: plane κ_0, icosphere κ_1, sphere κ_2, and mouse κ_3. The number of 0-, 1-, and 2-simplices found these simplicial complexes are tabulated in Table 1**Error! Reference source not found.**. Note that the blue and red colours in Figure 3 represent positive (+1) and negative (-1) constraints respectively.

ISBN: 978 0 994 3656 68

Table 1 Number of p-simplices found in the four simplical complexes.

p	κ_0	κ_1	κ_2	κ_3
0	4	42	482	846
1	5	120	1,440	2,532
2	2	80	960	1,688

Table 2 Time taken to generate hairs over the four simplicial complexes.

	κ_0	κ_1	κ_2	κ_3
Hairs	5,766	76,800	121,152	224,339
Time (s)	2.000	24.25	47.97	431.5

By observing the hair directional pattern of the 3D models in Figure 3, it is clear that hair directions reflect the constrained vector field. In the plane, hair directions follow the positively constrained edge, and oppose the negatively constrained edge. Vortices are formed from triangular constraints in the icosphere. As for the sphere, the hair directions begin from the source towards the sink. Furthermore, the generated hair directions are smooth, most obvious being the hair directional pattern on the multi-faceted geometry of the icosphere.

Figure 3: The four simplicial complexes and their vector fields satisfying the given constraints.

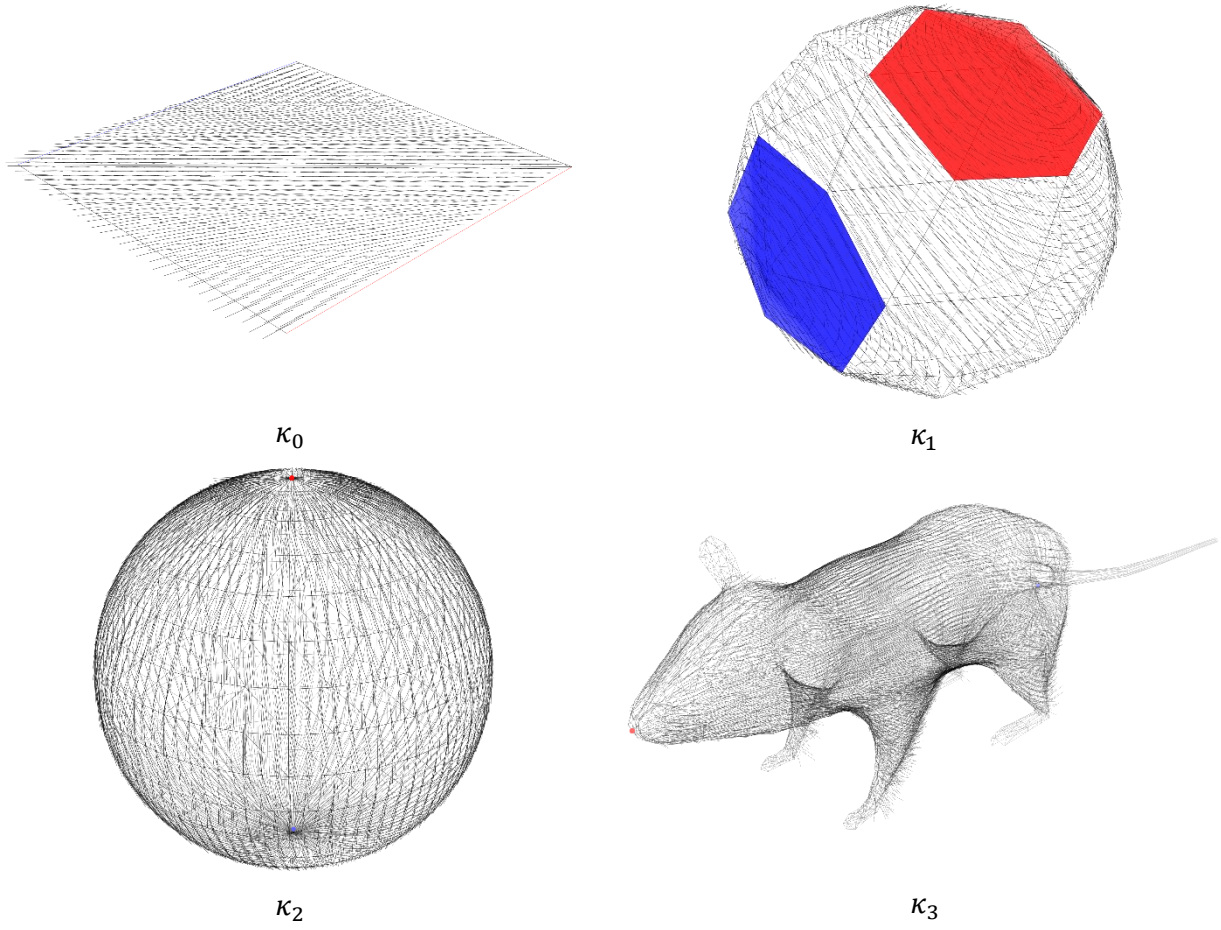

ISBN: 978 0 994 3656 68

Figure 4 Generated hair-like structures for κ_0, κ_1, and κ_2.

The time taken to generate hair coats for all four simplicial complexes is shown in Table 1**Error! Reference source not found.**. The mouse 3D model κ_3, being more complex has more vertices, edges and triangles than the other 3D models as shown in Table 1**Error! Reference source not found.**. The complexity of κ_3 in conjunction to its high total hair count contributed to the increase in time taken to generate the hair coat. Results of generating the hair coats on the first three simplicial complexes are shown in Figure 4**Error! Reference source not found.**. Note that the varying hair types in the plane made it appear like a patch of grass, the smooth hair directional pattern despite the hairs are rooted to a faceted surface in the icosphere, while the sphere looks like a hairy ball with its hairs smoothly combed along its surface from top to bottom.

Figure 5: Comparing hair coats from the proposed with one generated with a simple force field.

Proposed approach.

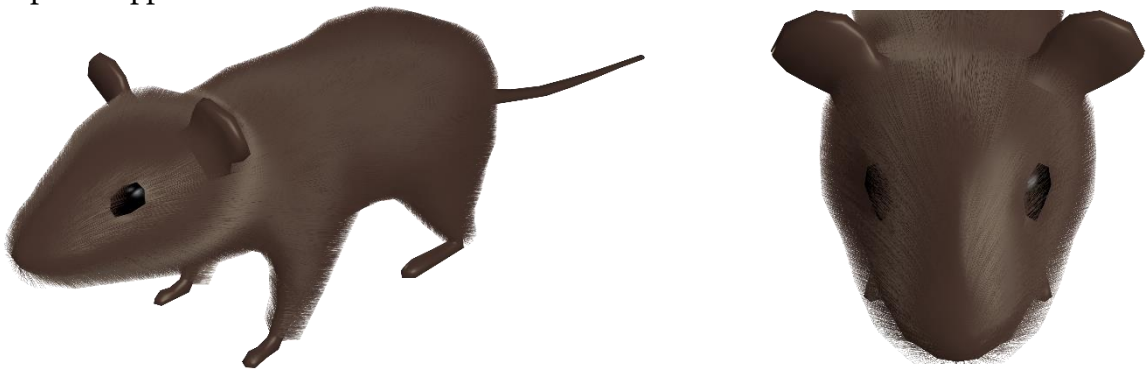

Control experiment.

ISBN: 978 0 994 3656 68

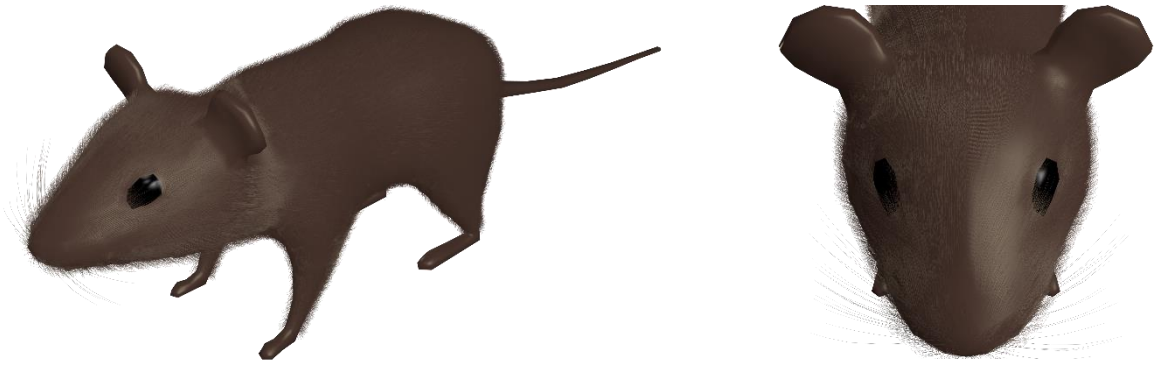

Proposed approach with shorter hair length.

Figure 5 shows the hair coat generated on κ_3 in comparison with a control experiment. Note how the hairs climb up the ears and the fuzzy silhouette of the hair coat generated using the proposed approach. Moreover, the different hair densities and lengths further contribute to the fuzziness of the hair coat, most prominently are the presence of whiskers. These properties are missing in the control experiment due to the absence of the four mouse hair types, mouse hair distributions mimicking natural ones, and that the wind force field does not act along the surface of the 3D model (Figure 3).

Figure 6 Comparing the generated hair coat of $\boldsymbol{\kappa_3}$ (top left) with overall hair directional pattern (top right) to a real mouse hair coat (bottom) reproduced from literature [21].

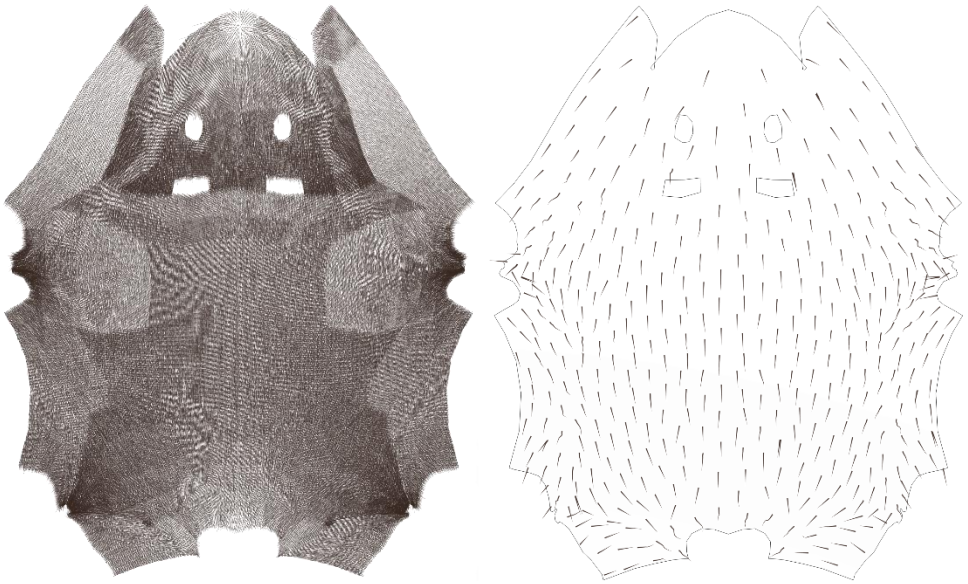

ISBN: 978 0 994 3656 68
www.apiar.org.au

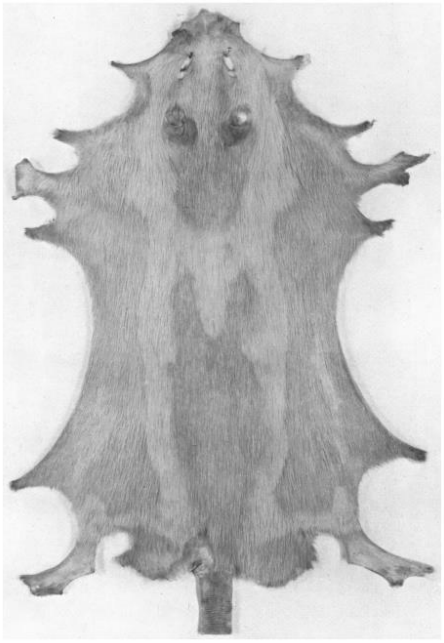

Finally, the generated hair coat is compared to a real mouse hair coat in **Error! Reference source not found.**. It is clear that the generated hair directional pattern follows that of a natural mouse coat, where the hair direction begins from the nose to the tail. Since only one hair distribution is generated for sampling repetitively over each body region of κ_3, a distinct change in hair density from one body region to another is revealed when the κ_3 is flattened in **Error! Reference source not found.**, although the generated hair coat on κ_3 appears natural in Figure 5. One possible solution is to apply a smooth transition between the borders of these areas to further enhance the appearance of a natural mouse coat.

Conclusion

In conclusion, the consequence of stretching of skin during hair development is imitated using an interpolated vector field determined by the user-defined placement of constraints on an arbitrary 3D model. Results show that the hair coat generated using this approach exhibits the same hair directions found naturally on wild-type mice in roughly 7 minutes. In addition, the inclusion of the four different mouse hair types has further enhanced the realism of the generated hair coat. Similarly, this approach can be used for all hair-like masses such as grass, thorns, feathers, scales, or synthetic fibres. Additional modification, physics simulation or animation can also be applied to the generated results. The clear advantages of this approach is that it models the consequence of the natural hair development process, in contrast to replicating the appearance of hair. Not only does this approach enable the generation of hair-like coats that closely resembles the ones found in nature with minimal user input and time, it can also be used for fictional creatures. In the future, the 2D interpolated vector field could be extended to 3D to accommodate for longer hair and more complex hairstyles.

References

[1] T. Schlake, "Determination of hair structure and shape," *Semin. Cell Dev. Biol.*, vol. 18, no. 2, pp. 267–273, Apr. 2007.
[2] J. H. Claxton, "The hair follicle group in mice," *Anat. Rec.*, vol. 154, no. 2, pp. 195–207, 1966.
[3] J. P. Parnell, "Hair Pattern and Distribution in Mammals," *Ann. N. Y. Acad. Sci.*, vol. 53, no. 3, pp. 493–497, 1951.
[4] J. H. Claxton, "The initiation and development of the hair follicle population in tabby mice," *Genet. Res.*, vol. 10, no. 02, pp. 161–171, 1967.
[5] S. Sick, S. Reinker, J. Timmer, and T. Schlake, "WNT and DKK Determine Hair Follicle Spacing Through a Reaction-Diffusion Mechanism," *Science*, vol. 314, no. 5804, pp. 1447–1450, Dec. 2006.
[6] S. M. Bong and S. Bangay, "Use of a Reaction-Diffusion Model to Generate Biologically Inspired Parameters for Synthetic Creatures," *Unpubl. Manuscr.*, 2015.
[7] K. Ward, F. Bertails, T.-Y. Kim, S. R. Marschner, M.-P. Cani, and M. C. Lin, "A Survey on Hair Modeling: Styling, Simulation, and Rendering," *IEEE Trans. Vis. Comput. Graph.*, vol. 13, no. 2, pp. 213–234, Mar. 2007.
[8] B. Choe and H.-S. Ko, "A statistical wisp model and pseudophysical approaches for interactive hairstyle generation," *IEEE Trans. Vis. Comput. Graph.*, vol. 11, no. 2, pp. 160–170, Mar. 2005.
[9] W. T. Reeves, "Particle Systems - a Technique for Modeling a Class of Fuzzy Objects," *ACM Trans Graph*, vol. 2, no. 2, pp. 91–108, Apr. 1983.
[10] M. Chai, L. Wang, Y. Weng, Y. Yu, B. Guo, and K. Zhou, "Single-view Hair Modeling for Portrait Manipulation," *ACM Trans Graph*, vol. 31, no. 4, pp. 116:1–116:8, Jul. 2012.
[11] L. Luo, H. Li, and S. Rusinkiewicz, "Structure-aware Hair Capture," *ACM Trans Graph*, vol. 32, no. 4, pp. 76:1–76:12, Jul. 2013.
[12] L. Hu, C. Ma, L. Luo, and H. Li, "Robust Hair Capture Using Simulated Examples," *ACM Trans Graph*, vol. 33, no. 4, pp. 126:1–126:10, Jul. 2014.
[13] S. Paris, W. Chang, O. I. Kozhushnyan, W. Jarosz, W. Matusik, M. Zwicker, and F. Durand, "Hair Photobooth: Geometric and Photometric Acquisition of Real Hairstyles," *ACM Trans Graph*, vol. 27, no. 3, pp. 30:1–30:9, Aug. 2008.
[14] T. L. Herrera, A. Zinke, and A. Weber, "Lighting Hair from the Inside: A Thermal Approach to Hair Reconstruction," *ACM Trans Graph*, vol. 31, no. 6, pp. 146:1–146:9, Nov. 2012.
[15] L. Wang, Y. Yu, K. Zhou, and B. Guo, "Example-based Hair Geometry Synthesis," *ACM Trans Graph*, vol. 28, no. 3, pp. 56:1–56:9, Jul. 2009.
[16] C. Yuksel, S. Schaefer, and J. Keyser, "Hair Meshes," *ACM Trans Graph*, vol. 28, no. 5, pp. 166:1–166:7, Dec. 2009.
[17] A. J. Weber and G. Gornowicz, "Collision-free Construction of Animated Feathers Using Implicit Constraint Surfaces," *ACM Trans Graph*, vol. 28, no. 2, pp. 12:1–12:8, May 2009.
[18] T. Beeler, B. Bickel, G. Noris, P. Beardsley, S. Marschner, R. W. Sumner, and M. Gross, "Coupled 3D Reconstruction of Sparse Facial Hair and Skin," *ACM Trans Graph*, vol. 31, no. 4, pp. 117:1–117:10, Jul. 2012.
[19] M. Fisher, P. Schröder, M. Desbrun, and H. Hoppe, "Design of Tangent Vector Fields," *ACM Trans Graph*, vol. 26, no. 3, Jul. 2007.
[20] M. Desbrun, E. Kanso, and Y. Tong, "Discrete Differential Forms for Computational Modeling," in *Discrete Differential Geometry*, A. I. Bobenko, J. M. Sullivan, P. Schröder, and G. M. Ziegler, Eds. Birkhäuser Basel, 2008, pp. 287–324.
[21] A. Durward and K. M. Rudall, "Studies on hair growth in the rat," *J. Anat.*, vol. 83, no. Pt 4, pp. 325–335, Oct. 1949.